Delivery of Phosphodiester Oligonucleotides: Can DOTAP/DOPE Liposomes Do the Trick?†

K. Remaut, B. Lucas, K. Braeckmans, N. N. Sanders, J. Demeester, and S. C. De Smedt*

Laboratory of General Biochemistry and Physical Pharmacy, Ghent University, Harelbekestraat 72, 9000 Ghent, Belgium

Received September 29, 2005; Revised Manuscript Received December 16, 2005

ABSTRACT: Delivering phosphodiester ONs (PO-ONs) remains an attractive but challenging goal in antisense therapy. Both in the literature and in our experiments, most cationic liposomes fail in generating an antisense effect with PO-ONs, while they succeed with chemically modified ONs such as phosphothioate ONs (PS-ONs). This work aims to explain the biological activity of PO- and PS-ONs delivered by DOTAP/DOPE liposomes based on a detailed understanding of their cell biological behavior by means of fluorescence correlation spectroscopy and confocal laser scanning microscopy. We conclude that DOTAP/DOPE liposomes are not suited to deliver PO-ONs due to the release of naked PO-ONs in the cytosol at the time of the endosomal escape of the liposomes and the subsequent rapid degradation of the naked PO-ONs. Carriers that would not release the PO-ONs upon endosomal escape but would continue to carry the PO-ONs until they arrive at the target mRNA could therefore be better suited to delivering PO-ONs. In the case of PS-ONs, the ONs are not degraded upon release at the time of the endosomal escape of the liposomes, creating a pool of intact, biologically active PS-ONs and thus making DOTAP/DOPE liposomes mainly suitable for delivering nuclease resistant ONs. However, the cells seemed to display an export pathway for removing intact PS-ONs from the cells, limiting the presence of naked PS-ONs in the nucleus to ∼8 h following the delivery.

Antisense ONs[1] show potential as therapeutics in the treatment of viral infections and cancer (*1*). Oligonucleotide-based therapeutics act by a sequence specific binding to their target mRNA, which results in blocking or degradation of the target sequence. This in turn results in the downregulation of the targeted protein expression. Despite this simple mechanism of action and many identified potential targets, no oligonucleotide-based therapeutics are actually on the market (*2*).

To improve the efficacy of ONs, chemically modified ONs are used to minimize the degradation in the body (*3*). The synthesis of modified ONs can however introduce unwanted side effects (*3*, *4*). Therefore, finding optimal delivery systems ("carriers") for unmodified phospodiester ONs (PO-ONs) remains attractive but very challenging. Generally speaking, optimal carriers for PO-ONs should protect the ONs against enzymatic degradation, enhance their cellular entry, and facilitate endosomal escape. The ONs should also be released into the cytoplasm of the cells or should be able to exert an antisense effect while being encapsulated by the carriers. Clearly, the carriers should be sufficiently "intelligent" to overcome extra- and intracellular barriers to be able to deliver sufficient amounts of intact PO-ONs at their target.

Cationic liposomes are among the most widely investigated carriers for delivery of nucleic acids (*5*). When cationic liposomes are mixed with the negatively charged ONs, spontaneously cationic liposome−ON complexes (lipoplexes) are formed. In literature as well as in our experiments, cationic liposomes fail to generate an antisense effect with PO-ONs, while they succeed with the chemically modified phosphothioate ONs (PS-ONs) (*6*−*8*). It is well-known that PS-ONs are more resistant to enzymatic degradation than ONs with a phosphodiester backbone. Therefore, a major hypothesis for explaining the difference in biological activity is that PS-ONs remain stable while PO-ONs degrade. However, to find better carriers for PO-ONs, one should know when and where in the cells the PO-ONs begin to degrade. Importantly, we should also know whether, besides degradation of the PO-ONs, other intracellular mechanisms are involved in limiting the biological activity of PO-ONs. This study aims to explain the biological activity of PO- and PS-ONs delivered by liposomes composed of the cationic lipid DOTAP and the neutral helper lipid DOPE, based on a detailed understanding of their intracellular fate. The liposome−ON complexes exhibited rapid cellular entry followed by a rapid endosomal escape with, importantly, release of naked ONs in the

† K.R. is a Research Assistant of the Research Foundation-Flanders (Flanders, Belgium). N.N.S. and K.B. are Postdoctoral Fellows of the Research Foundation-Flanders. The financial support of this institute is acknowledged with gratitude.

* To whom correspondence should be addressed: Laboratory of General Biochemistry and Physical Pharmacy, Ghent University, Harelbekestraat 72, 9000 Ghent, Belgium. Telephone: 0032-9-2648076. Fax: 0032-9-2648189. E-mail: stefaan.desmedt@ugent.be.

[1] Abbreviations: CLSM, confocal laser scanning microscopy; DOPE, dioleoylphosphatidylethanolamine; DOTAP, *N*-[1-(2,3-dioleoyloxy)-propyl]-*N*,*N*,*N*-trimethylammonium chloride; FCS, fluorescence correlation spectroscopy; FRET, fluorescence resonance energy transfer; ICAM, intracellular adhesion molecule; LPXs, lipoplexes; ONs, oligonucleotides; PEI, polyethyleneimine; *graft*-pDMAEMA, poly(2-dimethylamino)ethyl methacrylate-*co*-aminoethyl methacrylate-bearing polyethylene glycol chains; PO-LPXs, lipoplexes containing phosphodiester oligonucleotides; PO-ONs, phosphodiester oligonucleotides; PS-LPXs, lipoplexes containing phosphothioate oligonucleotides; PS-ONs, phosphothioate oligonucleotides; *R*/*G* ratio, ratio of the red to green fluorescence.

10.1021/bi0519755 CCC: $33.50
Published on Web 01/24/2006

cytoplasm of the cells. The PO-ONs released in the cytosol of the cells were rapidly degraded. Therefore, we suggest that cationic carriers that do not release the PO-ONs upon escape from the endosomes but continue to carry their cargo until they reach the target side in the cytosol would be more suitable for delivering nuclease sensitive PO-ONs. In contrast, the released PS-ONs stayed intact in the intracellular environment, creating a pool of biologically active PS-ONs. However, the cells seemed to display an export pathway for removal of intact PS-ONs, thus limiting the intracellular residence time of PS-ONs to ~8 h.

MATERIALS AND METHODS

Materials. Anti-ICAM-1 20mer ONs with a phosphodiester backbone (PO-ON) or a phosphothioate backbone (PS-ON) were used (Isis1939, 5′ CCC-CCA-CCA-CTT-CCC-CTC-TC 3′). For fluorescence correlation spectroscopy (FCS) experiments and confocal imaging, the anti-ICAM-1 ONs were doubly labeled with a rhodamine green fluorophore at the 3′ end (λ_{ex} = 488 nm, λ_{em} = 532 nm) and a Cy5 fluorophore at the 5′ end (λ_{ex} = 647 nm, λ_{em} = 670 nm). All ONs were purchased from Eurogentec (Seraing, Belgium) and were PAGE-purified by the supplier.

The cationic phospholipid DOTAP {*N*-[1-(2,3-dioleoyloxy)propyl]-*N*,*N*,*N*-trimethylammonium chloride} and the neutral phospholipid DOPE (dioleoylphosphatidylethanolamine) were purchased from Avanti Polar Lipids (Alabaster, AL).

Human lung carcinoma cells (A549 cells, ATCC number CCL-185) (DSMZ, Braunschweig, Germany) were cultured in Dulbecco's modified Eagle's medium (DMEM) without phenol red (Gibco, Merelbeke, Belgium) containing 2 mM glutamine, 10% heat-deactivated fetal bovine serum (FBS), and 1% penicillin-streptomycin at 37 °C in a humidified atmosphere containing 5% CO_2.

Preparation of Liposome−ON Complexes. The liposomes contained DOTAP and DOPE in a 1:1 molar ratio and were prepared as described elsewhere (*9*). The hydrodynamic size and ζ potential of the resulting cationic liposomes were routinely checked by dynamic light scattering (DLS, Malvern 4700 instrument, Malvern, Worcestershire, U.K.) and surface potential measurements (Zetasizer 2000 instrument, Malvern), respectively, as previously described (*10*) and equaled 126 ± 7 nm and 45 ± 4 mV, respectively.

Confocal Imaging and Fluorescence Correlation Spectroscopy (FCS). Confocal imaging and dual-color FCS experiments were performed on a Confocor2 instrument installed on a LSM510 confocal laser scanning microscope (Carl Zeiss, Jena, Germany). The excitation light of an argon ion laser (488 nm, 30 mW) and/or a helium−neon laser (633 nm, 5 mW) was reflected by a dichroic mirror (HFT 488/633) and focused through a Zeiss C-apochromat 40×, NA 1.2 water immersion objective into the sample. The fluorescence emission was re-collected by the same objective and split by another dichroic mirror (NFT 635) into the green detector (after passing through a 505−550 nm band-pass filter) or into the red detector (after passing through a 650 nm long-pass filter). Detection of the emission light was obtained with photon multipliers (in the case of confocal imaging) or much more sensitive avalanche photodiodes (in the case of FCS). Confocal detection was ensured by excluding out-of-plane fluorescence with pinholes in front of the detectors (70 or 90 μm for the green or red detector, respectively). For FCS measurements, the apparatus was calibrated by measuring the diffusion time of rhodamine green in solution, which equaled 40 ± 5 μs in this FCS setup and corresponds to a diffusion coefficient of 2.8×10^{-10} m^2/s.

When intracellular FCS measurements were performed, first a LSM510 confocal image of the cell was taken. Then, Confocor2 measuring points were selected on the confocal image in the cytoplasm or the nucleus of the cell, and the green and red fluorescence intensities were recorded with laser excitation set to 488 nm (or 633 nm). From these fluorescence intensities, the *R*/*G* ratio was calculated. When possible, the calculated autocorrelation curves $G(t)$ were analyzed with the Confocor2 software or in Origin (Originlab, Northampton, MA) using a single-species (eq 1) or dual-species (eq 2) fit according to the Marquardt nonlinear least-squares fit algorithm. This gives information about the amount of molecules (N) in the detection volume and their diffusion time (τ_t), being the average time the fluorescently labeled molecules need to migrate through the detection volume of the FCS instrument.

$$G(t) = 1 + \frac{1}{N}\left[1 - T + T\exp\left(\frac{-t}{\tau_T}\right)\right]\frac{1}{\left(1+\frac{t}{\tau_t}\right)\sqrt{1+\left(\frac{\omega_1}{\omega_2}\right)^2\left(\frac{t}{\tau_t}\right)}} \quad (1)$$

$$G(t) = 1 + \frac{1}{N}\left[1 - T + T\exp\left(\frac{-t}{\tau_T}\right)\right] \times \left[\frac{y}{\left(1+\frac{t}{\tau_{t1}}\right)\sqrt{1+\left(\frac{\omega_1}{\omega_2}\right)^2\left(\frac{t}{\tau_{t1}}\right)}} + \frac{1-y}{\left(1+\frac{t}{\tau_{t2}}\right)\sqrt{1+\left(\frac{\omega_1}{\omega_2}\right)^2\left(\frac{t}{\tau_{t2}}\right)}}\right] \quad (2)$$

where ω_1 and $2\omega_2$ represent the radius and the height of the detection volume, respectively, T represents the percentage of molecules in the triplet state, and τ_T represents the triplet relaxation time. For the dual-species fit (eq 2), there are Ny molecules with a diffusion time of τ_{t1} and $N(1-y)$ molecules with a diffusion time of τ_{t2}.

Transfection of A549 Cells with ON-Containing DOTAP/DOPE Liposomes. Lipoplexes (LPXs) were prepared by mixing 15 μL of a liposome dispersion (200 μM) and 15 μL of fluorescently doubly labeled ONs (2 μM), resulting in a +/− ratio of 5 (being the ratio of the number of positive charges, originating from the liposomes, to the number of negative charges, originating from the ONs). The resulting dispersion was vortexed for 10 s, and the lipoplexes were allowed to equilibrate for 30 min at room temperature prior to being used. Then, 120 μL of DMEM was added before the lipoplex dispersion was transferred to A549 cells grown to 90% confluence on glass-bottom cover slips (part PG-1.5-14-F, glass bottom 1.5, MatTek Corp.). After incubation for 4 h at 37 °C and 5% CO_2, the cells were washed and incubated further in DMEM containing 2 mM glutamine, 10% heat-deactivated FBS, and 1% penicillin-streptomycin. Confocal imaging and FCS measurements were performed 1, 2, 4, 8, and 12 h after the lipoplex dispersion had been applied to the A549 cells.

Microinjection. Microinjection experiments were performed with a Femtojet microinjector and an Injectman NI

2 micromanipulator (Eppendorf, Hamburg, Germany) coupled to the LSM510 confocal laser scanning microscope. All injections were performed in the cytoplasm of A549 cells. Immediately after injection, FCS measurements were carried out as described above in Confocal Imaging and Fluorescence Correlation Spectroscopy. Naked fluorescently doubly labeled ONs (2 μM) or a mixture of fluorescently doubly labeled ONs (2 μM) and nonlabeled ONs (20 μM) were injected. Upon microinjection, the concentration of the injected ONs is expected to be diluted ~30 times, yielding intracellular concentrations of 66 and 733 nM.

Antisense Activity of PO- and PS-ONs Containing DOTAP/DOPE Liposomes. The antisense activity of nonlabeled phosphodiester (PO) and phosphothioate (PS) anti-ICAM-1 ONs was determined by detecting the ICAM-1 expression on the surface of A549 cells using an ELISA. Mycoplasma free A549 cells were plated onto 96-well microtiter plates at a density of 10^4 cells/well. At 90% confluency, the cells were washed three times with phosphate-buffered saline (PBS) (Gibco), and free or complexed ONs were added to the cells (0.7 μg of ON/well), followed by incubation for 4 h. Lipoplexes with +/− ratios of 2.5, 5, and 10 were used, containing nonlabeled ONs. Subsequently, the free or complexed ONs were removed, and after the cells had been washed with PBS, 100 μL of culture medium supplemented with 10 ng/mL TNF-α was added to induce overexpression of ICAM-1. After incubation for 18 h, the level of ICAM-1 expression was determined as described below. To determine the basal level of ICAM-1 expression, the cells were incubated for 18 h with 100 μL of culture medium without TNF-α.

ICAM-1 Assay. The cells were fixed for 15 min at room temperature with PBS containing 20 mg/mL paraformaldehyde. After the cells had been washed with PBS, aspecific binding places were blocked by incubating the cells for 1 h with 2% normal goat serum (NGS) in a 1% bovine serum albumin/PBS (BSA/PBS) solution. The cells were washed with PBS and incubated for 90 min at 37 °C with mouse anti-human ICAM-1 antibody (ImmunoSource, Zoersel, Belgium) (0.5 μg/mL in 1% BSA/PBS). After the cells had been washed with PBS, the amount of antibody bound to the cell surface was determined by incubating the cells for 1 h at 37 °C with a sheep anti-mouse antibody−alkaline phosphatase conjugate (1/1000 dilution in 1% BSA/PBS). After three washes, the alkaline phosphatase activity was determined using 100 μL of *p*-nitrophenyl phosphate [10 mg/mL in 0.1 M Tris (pH 8.4)]. After incubation for 30 min at 37 °C, the absorbance was determined using an ELISA plate reader at 405 nm (Wallac Victor2 multilabel reader, Perkin-Elmer Life Sciences, Boston, MA).

The antisense activity of the anti-ICAM-1 PO- or PS-ONs was calculated as the percentage of the ICAM-1 expression when compared to A549 cells that were treated with a control ON using eq 3. In this way, the levels of the basal and induced expression of the ICAM-1 protein in A549 cells treated with the control ON are set to 0 and 100%, respectively. As the level of the basal or induced expression can be influenced by the conditions to which the cells are subjected, the levels of basal and induced ICAM-1 expression were determined on cells that were treated with the control ON under the same conditions that were applied for the antisense PO- or PS-ONs (e.g., naked or complexed to DOTAP/DOPE liposomes at a +/− ratio of 2.5, 5, or 10).

$$\frac{(A_{\mathrm{ON,TNF-\alpha}} - A_{\mathrm{Control,CM}})}{(A_{\mathrm{Control,TNF-\alpha}} - A_{\mathrm{Control,CM}})} \times 100 \qquad (3)$$

where $A_{\mathrm{Control,CM}}$ is the absorption of cells treated with naked or complexed control ONs and without TNF-α induction (i.e., the basal level of ICAM-1 expression), $A_{\mathrm{Control,TNF-\alpha}}$ is the absorption of cells treated with naked or complexed control ONs upon induction with TNF-α (i.e., the control level of TNF-α-induced ICAM-1 expression), and $A_{\mathrm{ON,TNF-\alpha}}$ is the absorption of cells treated with naked or complexed anti-ICAM-1 ONs upon induction with TNF-α (i.e., the level of ON-treated TNF-α-induced ICAM-1 expression). As a control ON, an ON without anti-ICAM-1 activity was used (5′ GAG-ACT-TTC-ACT-TTT-CTC-TA 3′).

RESULTS

Anti-ICAM-1 Activity of Phosphodiester and Phosphothioate ONs Delivered by DOTAP/DOPE Liposomes. Figure 1 shows the antisense activity obtained with DOTAP/DOPE liposomes containing 20mer anti-ICAM-1 ONs with either a nuclease sensitive phosphodiester backbone (PO-ONs) or a nuclease stable phosphothioate backbone (PS-ONs). Naked PO- and PS-ONs did not exhibit antisense activity. It is indeed well-known that naked ONs do not adequately enter cells, which is often attributed to their negative charge. The antisense effect of LPXs with a +/− ratio of 2.5 does not differ significantly from the antisense effect established by naked ONs. In a previous study, we showed experimentally that at a +/− ratio of 2.5, only 45% of the ONs were complexed to the cationic liposomes, while the other part of the ONs remained free (*11*). Apparently, this inadequate complexation resulted in a low biological activity of the LPXs at this +/− ratio, for both PO- and PS-ONs. At a +/− ratio of 5 or 10, we previously showed that the amount of complexed ONs increased to 84 or 98%, respectively (*11*). In the case of PS-ONs, increasing the +/− ratio to 5 or 10 resulted in a significant antisense effect. PO-ONs however were not able to downregulate the targeted protein expression. A major difference between PO- and PS-ONs is the nuclease sensitivity of the backbone. Therefore, intracellular degradation could well be one of the factors limiting the antisense activity of the PO-ONs. In the following experiments, we aimed to figure out whether intracellular degradation is indeed the major barrier toward DOTAP/DOPE liposome-mediated PO-ON delivery or whether also other intracellular barriers contribute to the lack of antisense activity. Therefore, the intracellular pathway of fluorescently doubly labeled ONs complexed to DOTAP/DOPE liposomes was followed by FCS and confocal imaging.

Detection of Intact and Degraded ONs by FRET-FCS. In the intact fluorescently doubly labeled ONs, fluorescence resonance energy transfer (FRET) occurs between the rhodamine green (donor) and the Cy5 (acceptor) fluorophore (*12*). Consequently, excitation of rhodamine green gives rise to emission by both rhodamine green and Cy5 (Figure 2A, inset). A prerequisite for energy transfer is the proximity of the donor and acceptor fluorophore. When the ONs degrade, the distance between both fluorophores increases and FRET no longer occurs. Thus, excitation of the rhodamine green does not result in emission by the Cy5 (inset of Figure 2C). As outlined below, FRET can be used to distinguish between intact and degraded ONs.

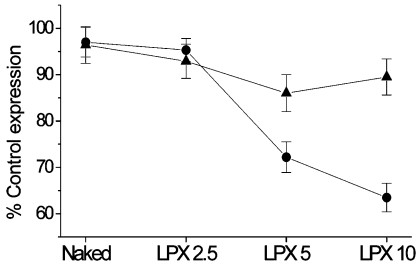

FIGURE 1: Antisense activity of phosphodiester ONs (▲) or phosphothioate ONs (●) administered to A549 cells naked or complexed to DOTAP/DOPE liposomes (LPX) at a +/− ratio of 2.5, 5, or 10. The antisense activity was calculated as the percentage of induced ICAM-1 expression when compared to A549 cells that were treated with the corresponding formulation containing the control ON (e.g., naked or complexed to DOTAP/DOPE liposomes at a +/− ratio of 2.5, 5, or 10) as described in Materials and Methods.

Figure 2A shows the fluorescence fluctuations as registered by the green and red detector of the FCS instrument upon excitation of a solution of intact doubly labeled ONs with 488 nm light. Clearly, the fluorescence intensity fluctuates as fluorescently labeled molecules move in and out of the detection volume of the FCS instrument. Because of FRET, the ONs are, besides green fluorescent, also red fluorescent.

Table 1: Fluorescence Intensities As Measured by the Green (F_G) and Red (F_R) Detector of the FCS Instrument for Solutions of Intact PS-ONs, Intact PO-ONs, and Degraded PO-ONs (488 nm light laser excitation)[a]

	intact PS-ONs	intact PO-ONs	degraded PO-ONs
F_R (kHz)	3.4	3.5	1.2
F_G (kHz)	1.4	2	8.8
R/G ratio	2.4	1.8	0.1
diffusion time τ_t (μs) as calculated from F_R	131 ± 6	125 ± 14	ND[b]
diffusion time τ_t (μs) as calculated from F_G	105 ± 12	110 ± 5	60 ± 5

[a] The R/G ratio represents the ratio of the red to green fluorescence. The diffusion times (τ_t) calculated from the autocorrelation curves obtained from these fluorescence fluctuations are depicted as well. The concentration of the ONs in solutions ranged between 5 and 10 nM. PO-ON hydrolysis was accomplished by incubating the intact PO-ONs with 20 units of the DNase II enzyme (4.7 units/μL, Sigma) for 8 h at 37 °C in an acidic buffer [40 mM acidic acid and 60 mM potassium acetate (pH 4.7)]. [b] Could not be determined.

Table 1 shows the "R/G ratio" which is defined as the ratio of the red to the green fluorescence as measured by the FCS detectors. For the intact doubly labeled ONs used in this study, the R/G ratio is greater than 1. Figure 2B shows that

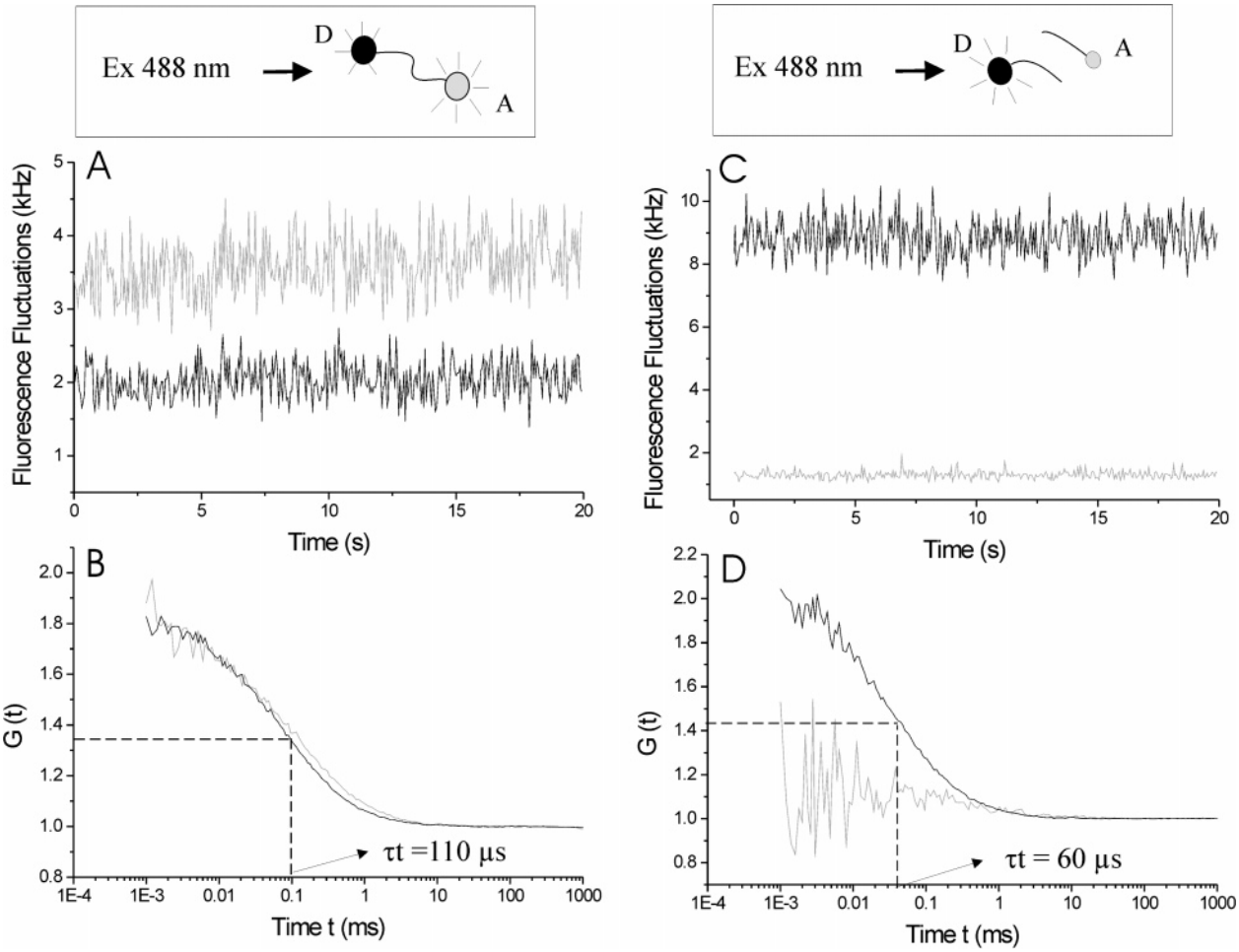

FIGURE 2: Schematic representation of FCS experiments on intact (inset in panel A) and degraded (inset in panel C) doubly labeled ONs. In the intact ONs, FRET occurs between rhodamine green (donor, D, black) and Cy5 (acceptor, A, gray) upon excitation with 488 nm laser light. Fluorescence fluctuations as registered by the green (black line) and red (gray line) detector of the FCS instrument in a solution of intact (A) and degraded (C) PO-ONs. Autocorrelation curves as obtained from the fluorescence fluctuations of intact (B) and degraded (D) PO-ONs. The concentration of the ONs in solutions ranged between 5 and 10 nM. PO-ON hydrolysis was accomplished by incubating the intact PO-ONs with 20 units of the DNase II enzyme (4.7 units/μL, Sigma) for 8 h at 37 °C in an acidic buffer [40 mM acidic acid and 60 mM potassium acetate (pH 4.7)].

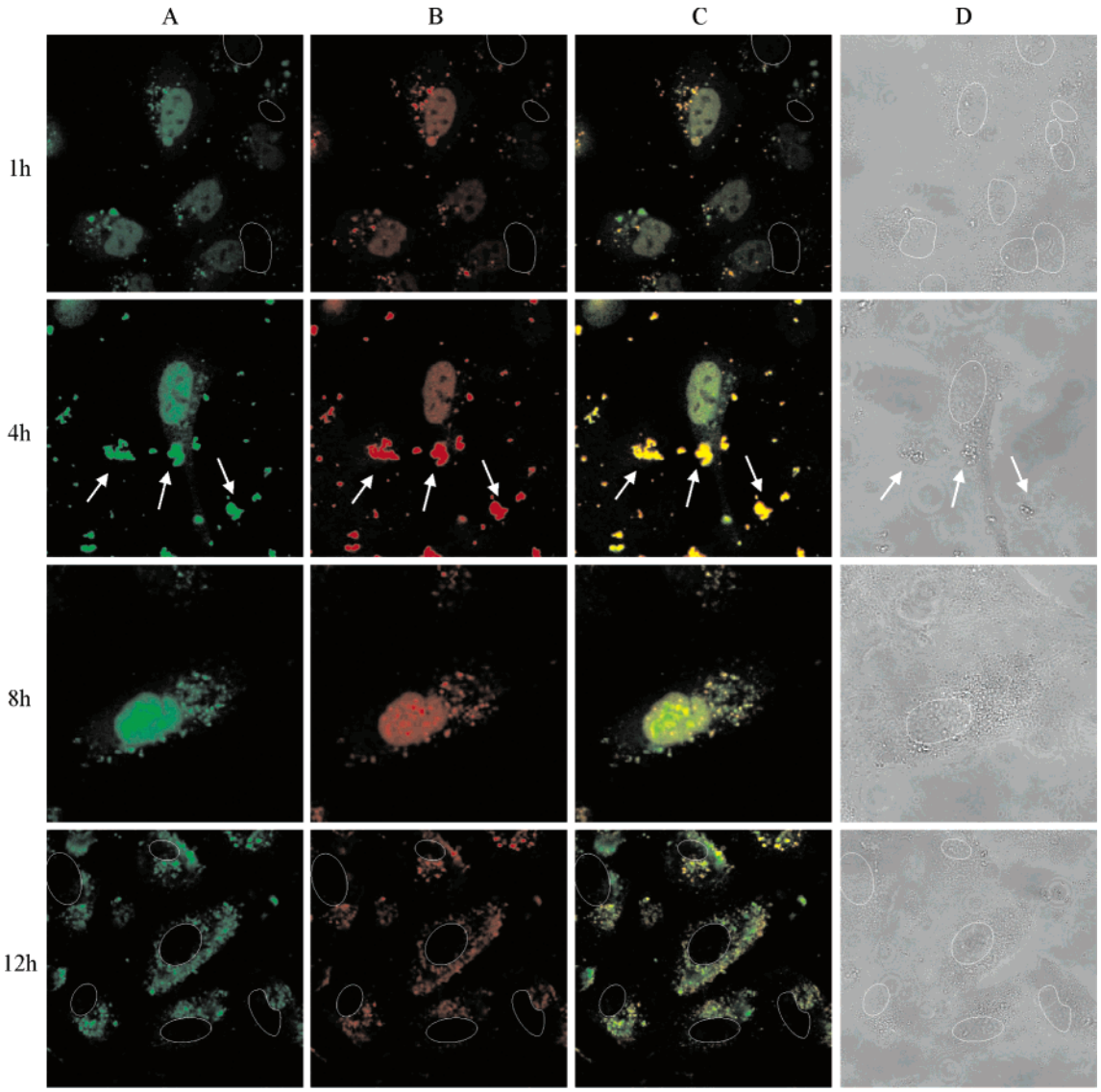

FIGURE 3: Green (A), red (B), and merged (C) confocal images of A549 cells 1, 4, 8, and 12 h after transfection with PS-LPXs. As 488 nm excitation light was used, the red fluorescence in panel B comes from Cy5 excitation due to FRET. In the transmission images (D), a circle was drawn around the nucleus (and also around the nonfluorescent nuclei in panels A−C). The arrows point to PS-LPX aggregates.

proper autocorrelation curves can be derived from both the green and red fluorescence fluctuations. The diffusion time, which is the average time the ONs need to migrate through the detection volume of the FCS instrument, can be calculated by fitting the autocorrelation curves to eq 1 (Table 1).

Figure 2C shows the fluorescence fluctuations as registered by the green and red detector upon excitation of a solution of degraded ONs with 488 nm light. Due to the disappearance of FRET, the Cy5 fluorophores can no longer be excited with 488 nm light. This is reflected in a decrease in the red fluorescence intensity in combination with an increase in the green fluorescence intensity, which lowers the *R*/*G* ratio (Table 1). Figure 2D shows that a proper autocorrelation curve can be obtained from the green fluorescence fluctuations and a diffusion time can be calculated by fitting to eq 1 (Table 1). In contrast, the red fluorescence fluctuations can no longer be autocorrelated. The latter together with the *R*/*G* ratio allows us to distinguish between intact and degraded doubly labeled ONs with the FCS instrument.

Intracellular Fate of Phosphothioate ONs Delivered by Cationic DOTAP/DOPE Liposomes. A549 cells were transfected with DOTAP/DOPE liposomes containing fluorescently doubly labeled phosphothioate ONs (PS-LPXs). At certain time points, confocal images were taken and FCS measurements were performed in the nucleus and cytoplasm of the cells with laser excitation set to 488 nm. In that case, excitation of the Cy5 fluorophores occurs only if the ONs are still intact.

Within 1 h of addition of PS-LPXs to A549 cells, confocal images showed green fluorescence in the nuclei of most cells (Figure 3A-1h). As the PS-LPXs themselves are by far too large (~150 nm) to cross the pores of the nuclear membrane, the nuclear fluorescence indicates the entry of free PS-ONs after they are released from the LPXs. Figure 3B-1h shows that red fluorescence can also be detected in the nuclei of most cells, indicating that FRET occurs and thus that the PS-ONs are intact. From the red and green fluorescence fluctuations in the nucleus, as measured by the FCS detectors (upon excitation at 488 nm), an average *R*/*G* ratio of 2.2 ± 0.4 was calculated, which agreed well with the *R*/*G* ratio of intact PS-ONs in buffer (Table 1). Also, proper autocorrelation curves could be generated from both the green and red fluorescence fluctuations (Figure 4). As we previously described (*12*), the diffusion time itself (as obtained from

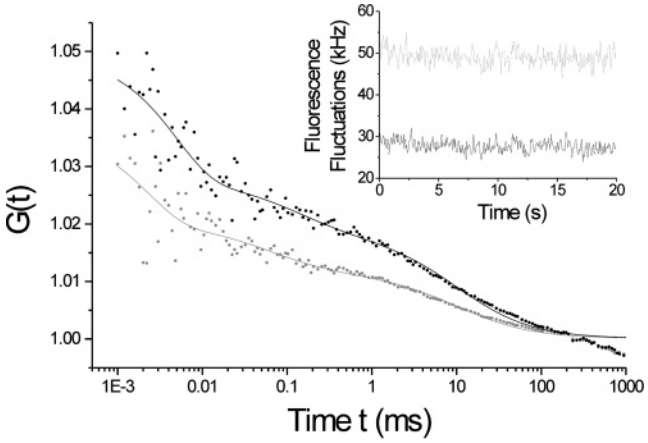

FIGURE 4: FCS measurements performed in the nucleus of A549 cells 1 h after transfection with PS-LPXs with 488 nm laser excitation. The graph shows the autocorrelation curves (···) as derived from the green (rhodamine green, donor) (black line) and red (Cy5, acceptor) (gray line) detector of the FCS instrument. The autocorrelation curves were best fitted with a two-component fit (eq 2) (—). The inset shows the green (black line) and red (gray line) fluorescence fluctuations from which the autocorrelation curves were derived.

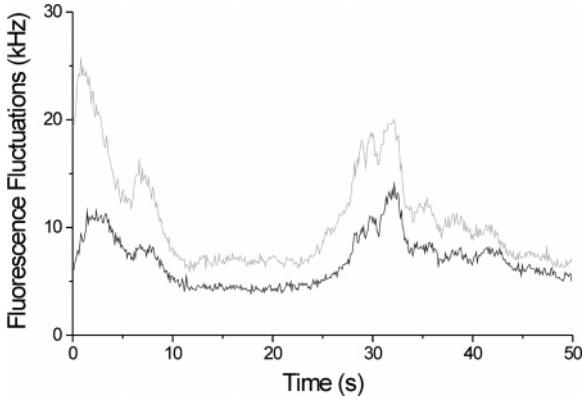

FIGURE 5: Fluorescence fluctuations as measured by the green (black line) and red (gray line) detector in the cytoplasm of A549 cells transfected with PS-LPXs. Laser excitation was set at 488 nm. The average *R*/*G* ratio of the fluorescence peaks was 1.6 ± 0.3, indicating intact ONs.

the autocorrelation curves) cannot be used to distinguish between intact and degraded doubly labeled ONs. Nevertheless, the fact that a proper autocorrelation curve can be derived for the Cy5 fluorophores upon 488 nm excitation points out that FRET still occurs. Therefore, we chose to depict the autocorrelation curves, which were best fitted with a two-component fit (eq 2), without further discussing the obtained diffusion times. Taken together, the above-mentioned observations clearly show that 1 h after transfection PS-ONs were released from the LPXs and stayed intact in the intracellular environment.

More PS-LPXs were able to enter the cells and release their ONs with the 4 h incubation time, as was concluded from the increased nuclear fluorescence intensity (Figure 3-4h). Also, as denoted by the arrows, aggregates of PS-LPXs became visible in the medium surrounding the cells. It is indeed known that lipoplexes have the tendency to aggregate into large multimolecular complexes at longer contact times (*13*). Figure 3B-4h indicates the presence of FRET in the PS-LPX aggregates outside the cells as well as in the free PS-ONs in the nuclei of the cells. Also here, the average *R*/*G* ratio of 2.3 ± 0.4 in the nuclei revealed that the PS-ONs were still intact.

With longer incubation times, the formation of nuclear bodies could be seen in some cells as bright fluorescent spots in the nucleus (Figure 3-8h). This phenomenon has been reported previously for PS-ONs, especially at higher concentrations (*14*−*16*). The nuclear bodies contained intact PS-ONs, as they were both green and red in color. Also, the *R*/*G* ratio of 1.8 ± 0.2 as measured in the nucleus demonstrates that the PS-ONs were still intact with an 8 h residence time.

After 12 h, the nuclear fluorescence largely disappeared (Figure 3-12h). The average fluorescence intensities in the nuclei, as measured by the FCS detectors, equaled the autofluorescence of the nuclei (∼5 kHz). Since the FCS detectors are much more sensitive than the CLSM detectors and can detect single molecules, this confirms that no PS-ONs are left in the nuclei of most cells. Importantly, the disappearance of PS-ONs from the nuclei correlated with the appearance of punctated structures in the cytoplasm of the cells (Figure 3A-12h). As seen from the red fluorescence in Figure 3B-12h, these cytoplasmic granules contain intact PS-ONs. Now and then, highly intense green and red fluorescence peaks simultaneously occurred in the fluorescence fluctuation profiles as measured by the FCS instrument in the cytoplasm of these cells (Figure 5). The fluorescence peaks had an average *R*/*G* ratio of 1.6 ± 0.3 and indicate the simultaneous movement of a number of intact PS-ONs through the detection volume of the FCS instrument. As deducted from the broadness of the peaks in Figure 5, the PS-ONs containing structures need ∼5−10 s to pass through the detection volume of the FCS instrument, indicating a slow movement in the cytosol.

Intracellular Fate of Phosphodiester ONs Delivered by Cationic DOTAP/DOPE Liposomes. A549 cells were transfected with DOTAP/DOPE liposomes containing fluorescently doubly labeled phosphodiester ONs (PO-LPXs). Like for the PS-LPXs, confocal images of the cells were taken and FCS measurements were performed in the nucleus and cytoplasm of the cells with the laser excitation set to 488 nm.

Green fluorescent nuclei were observed in the first hour after transfection (Figure 6A-1h). This demonstrates the entry of PO-LPXs into the cells and the release of the ONs from the LPXs, as only free ONs can diffuse through the pores of the nuclear membrane. In contrast to the case for PS-ONs (Figure 3), no red fluorescence was found in the nuclei upon excitation with 488 nm light (Figure 6B-1h). This suggests that FRET does not occur and indicates that the ONs present in the nuclei are degraded. FCS measurements in the nuclei revealed an average *R*/*G* ratio of 0.3 ± 0.1, showing that the released ONs that had entered the nuclei were indeed degraded. Also, upon excitation with 488 nm light, the autocorrelation curve obtained from the nuclear green fluorescence fluctuations (likely rhodamine green) was of good quality (Figure 7, black line) while the red fluorescence fluctuations (likely Cy5) could not be correlated (Figure 7, gray line). Nevertheless, red fluorescence could be detected in the PO-LPXs outside the cells (Figure 6B-1h, region 1) as well as in some PO-LPXs in the cytoplasm of the cells (Figure 6B-1h, region 2). By positioning the measuring points of the FCS instrument on the fluorescent dots, we could

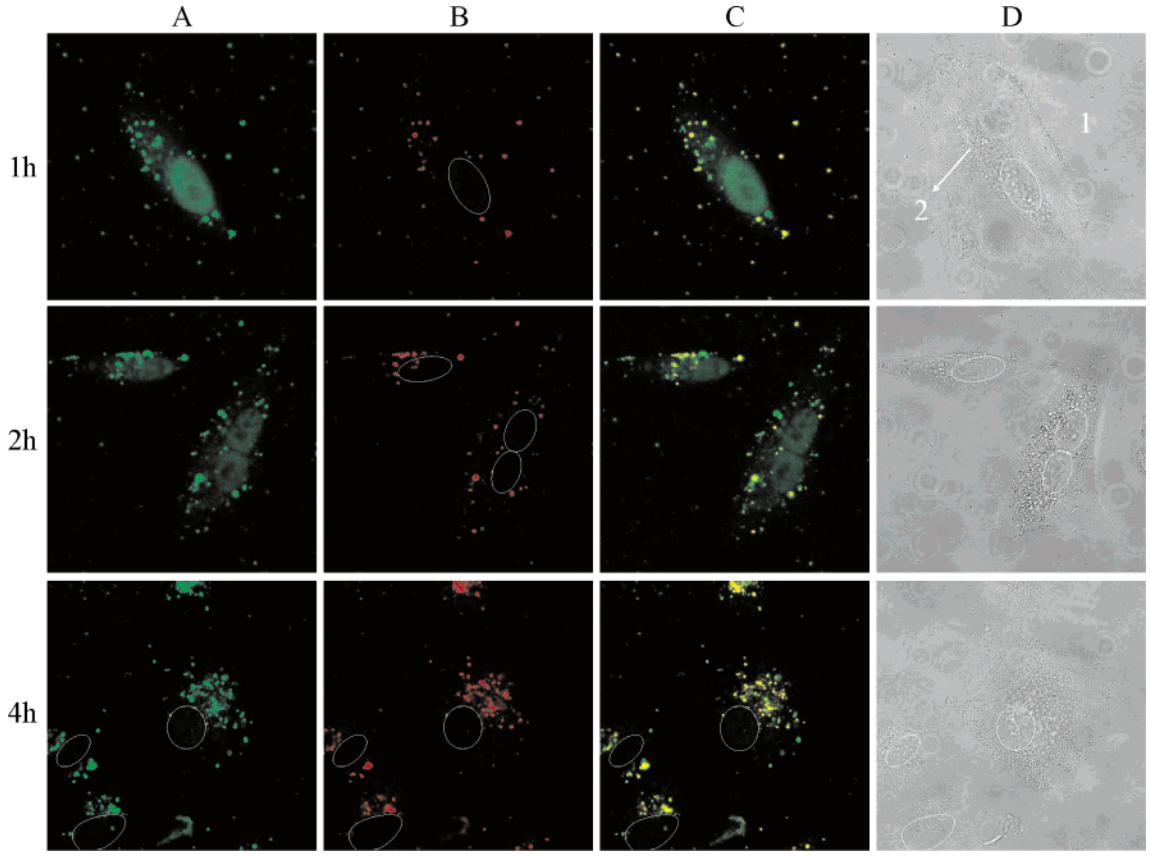

FIGURE 6: Green (A), red (B), and merged (C) confocal images of A549 cells 1 and 2 h after transfection with PO-LPXs. As 488 nm excitation light was used, the red fluorescence comes from Cy5 excitation due to FRET. In the transmission images (D), a circle was drawn around the nucleus (and also around the nonfluorescent nuclei in panels A−C).

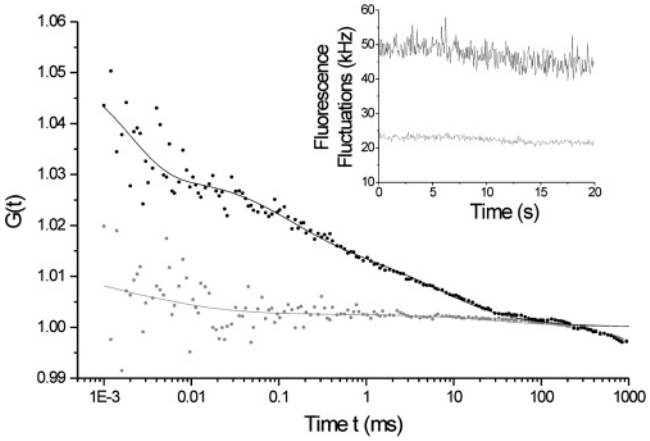

FIGURE 7: FCS measurements performed in the nucleus of A549 cells 1 h after transfection with PO-LPXs with 488 nm laser excitation. The graph shows the autocorrelation curves (···) as derived from the green (rhodamine green, donor) (black line) and red (Cy5, acceptor) (gray line) detector of the FCS instrument. The autocorrelation curves were best fitted with a two-component fit (eq 2) (—). The inset shows the green (black line) and red (gray line) fluorescence fluctuations from which the autocorrelation curves were derived.

determine the *R*/*G* ratio of the PO-LPXs. The average *R*/*G* ratio of the fluorescent dots in region 2 was 1.7 ± 0.2 and confirmed that the DOTAP/DOPE liposomes in the cytosol still contained intact PO-ONs, indicating that the degradation of the ONs occurs after release of the ONs from the LPXs.

The nuclear green fluorescence faded after incubation for 2 h (Figure 6A-2h) and disappeared with incubation times longer than 4 h (Figure 6A-4h). Most likely, as previously observed by Fisher et al. (*16*), the small fluorescent degradation products easily diffuse out of the cells and are therefore no longer detected. However, the red dots in Figure 6B-2h and Figure 6B-4h show that most of the LPXs in and around the cells still contain intact PO-ONs, again confirming that degradation mainly occurs after release of the PO-ONs from the LPXs.

Degradation of Naked Phosphodiester ONs upon Microinjection in A549 Cells. As described above, FCS measurements and confocal images of A549 cells transfected with DOTAP/DOPE liposomes revealed that PO-ONs were degraded in the intracellular environment within the first hour following transfection. Also, the data suggested that the degradation occurred after the PO-ONs were released from the liposomes. To see whether PO-ONs indeed degrade that rapidly, naked PO-ONs were injected in the cytoplasm of A549 cells and FCS measurements were performed to monitor the degradation.

As observed previously by others, PO-ONs accumulated in the nuclei of the injected cells within a few minutes of the injection (data not shown) (*17*, *18*). Despite this rapid nuclear accumulation, intact ONs could not be detected in the nuclei of the injected cells. This could be concluded from the *R*/*G* ratio of 0.3 ± 0.1. Also, a proper autocorrelation curve could not be registered from the red fluorescence fluctuations (acceptor) upon 488 nm excitation (Figure 8A, gray line), while a good autocorrelation curve could be obtained from the green fluorescence fluctuations (donor) (Figure 8A, black line). Subsequently, the concentration of the injected ONs was increased 11-fold after injection of a mixture of fluorescently labeled (2 μM) and nonlabeled ONs

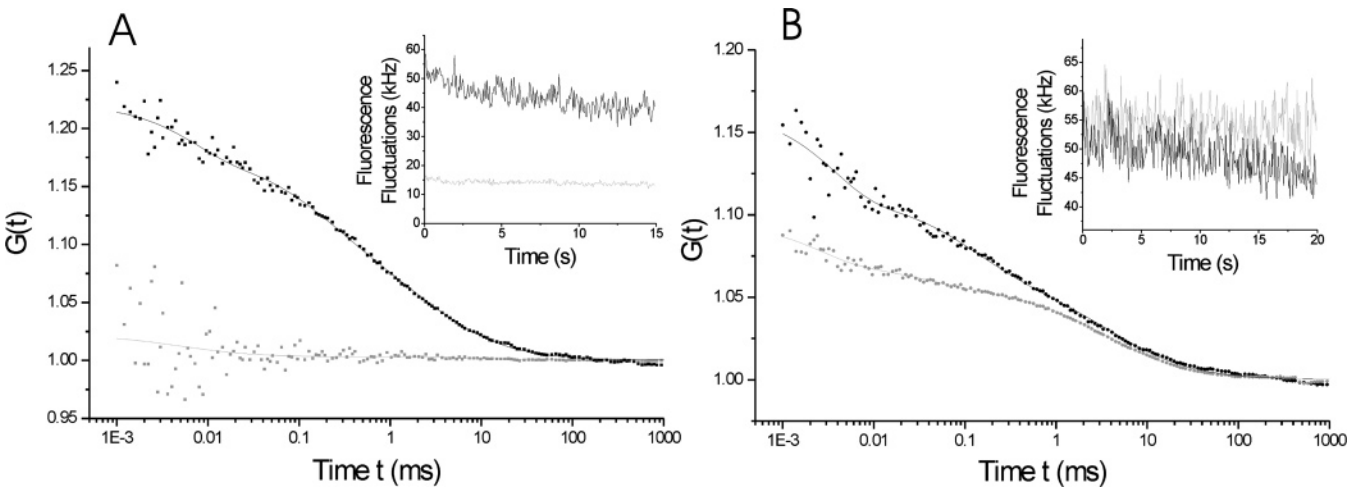

FIGURE 8: FCS measurements performed in the nucleus of A549 cells immediately after injection of (A) 2 μM fluorescently labeled PO-ONs and (B) a mixture of 2 μM fluorescently labeled and 20 μM nonlabeled PO-ONs. Injections were performed in the cytoplasm of A549 cells. The graph shows the autocorrelation curves (•••) as derived from the green (rhodamine green, donor) (black line) and red (Cy5, acceptor) (gray line) detector of the FCS instrument. The autocorrelation curves were best fitted with a two-component fit (eq 2) (—). The inset shows the green (black line) and red (gray line) fluorescence fluctuations from which the autocorrelation curves were derived.

(20 μM) in the cells. In that way, the amount of fluorescent ONs was kept sufficiently low to allow for proper autocorrelation analysis. As shown in Figure 8B, proper autocorrelation curves from both the green and red fluorescence fluctuations could be obtained upon excitation with 488 nm light, indicating that FRET occurred and thus intact ONs were present in the nuclei of the cells. Also, the *R*/*G* ratio of 1.1 ± 0.1 confirmed that intact ONs entered the nuclei when a larger amount of ONs was injected into the cytosol.

DISCUSSION

For some years now, antisense ONs have been investigated for the selective inhibition of various genes (*1*). Regretfully, the therapeutic potential remains largely unrealized. Attempts to fundamentally explain the biological activity of nucleic acid-loaded carriers, by studying their biophysical properties and cell biological behavior, are scarce, although these studies are greatly needed to allow the design of better delivery systems for nucleic acids. For that purpose, our laboratory uses advanced microscopy techniques such as fluorescence correlation spectroscopy (*19*−*21*). In this work, we studied the intracellular pathway of ONs with a phosphodiester (PO-ONs) or a phosphothioate (PS-ONs) backbone delivered by DOTAP/DOPE liposomes with the focus on the intracellular degradation of the ONs.

It is widely accepted that liposomes predominantly enter cells by endocytosis (*22*−*25*). Upon endocytosis of the DOTAP/DOPE liposomes loaded with fluorescent ONs, one would expect to see the endosomal vesicles as fluorescent dots in the cytoplasm of the transfected cells. Surprisingly, rather few cytoplasmic fluorescent dots were detected in the first hour following transfection. In contrast, fluorescent nuclei were observed within the first hour after application of the lipoplexes (LPXs) to the A549 cells. These observations suggest that the endosomal escape of the DOTAP/DOPE liposomes and release of the ONs in the cytosol of the A549 cells is a very efficient process. A possible mechanism for endosomal escape of ON-containing lipoplexes has been proposed by Zelphati and Szoka (*26*). According to these authors, lipid contact occurs between cationic lipids from the lipoplex and anionic lipids from the inner face of the endosomal membrane, resulting in flip-flop of anionic lipids from the cytoplasmic face of the endosomal membrane. These anionic lipids laterally diffuse into the lipoplex and form a charged neutralized ion pair with the cationic lipids from the lipoplexes, which results in destabilization of the lipoplexes and displacement of the negatively charged ONs with their release into the cytoplasm of the cells. Recently, Gordon et al. (*27*) demonstrated that anionic lipids in the endosomal membrane are not a primary prerequisite to trigger ON release. In contrast, neutral helper lipids in the delivery system, such as DOPE, seem to play a crucial role in improving the endosomal escape by adopting a hexagonal phase in the lumen of the endosomes that destabilizes the endosomal membrane (*28*, *29*). Therefore, the presence of DOPE in the liposome formulation used in this study should explain the rapid endosomal escape that results in release of the ONs in the cytoplasm of the transfected cells.

Several studies have reported that, once in the cytosol, free ONs readily accumulate in the nucleus (*15*, *17*, *18*) while the larger DOTAP/DOPE liposomes remain in the cytoplasm (*24*, *30*). Via FCS, we observed that the ONs present in the nuclei were intact in the case of phosphothioate ONs (PS-ONs) but degraded in the case of phosphodiester ONs (PO-ONs). It is well-known that PS-ONs are more resistant to degradation by nucleases. However, lifetimes of PO-ONs in cells reported in the literature vary from minutes to some hours (*16*, *17*, *31*, *32*). In this study, we found that injected PO-ONs were degraded within minutes when injected at low concentrations (2 μM), while intact PO-ONs could be detected when the injected concentration was 11-fold higher. The fact that intact PO-ONs were not observed in the nuclei of the transfected cells, together with the observation that intact PO-ONs were detected in the PO-LPXs outside as well as inside the transfected cells, suggests that degradation occurs after release of the PO-ONs from the DOTAP/DOPE liposomes. We indeed demonstrated previously that DOTAP/DOPE liposomes offer beneficial protection against enzymatic degradation to the PO-ONs they are carrying, as long

as the PO-ONs remain complexed to their carrier (*11*). Nevertheless, this study demonstrates that this protection against enzymatic degradation does not translate into a biological effect due to the excessively efficient release and subsequent degradation of the PO-ONs at the termination of endosomal escape. We additionally observed that the nuclear fluorescence faded within the first 2 h after PO-ONs containing LPXs had been exposed to the A549 cells. This probably reflects the diffusion of the shorter fluorescent degradation products out of the cells, as observed previously by Fisher et al. (*16*). It should be noted that the fluorescent labels at the 3′ and 5′ ends of the doubly labeled ONs could interfere with the splicing activity of exonucleases. Therefore, the actual degradation of unlabeled ONs is expected to occur even more rapidly.

In the case of phosphothioate ONs, intact PS-ONs could be observed in the nuclei of the cells for at least 8 h. This was no surprise as the more stable PS-ONs are not expected to degrade upon their release at the time of endosomal escape, thus creating a pool of intact PS-ONs. This in turn results in a longer time for PS-ONs to bind to the target mRNA and to inhibit the targeted protein expression, which most likely explains why the nuclease stable phosphothioate ONs could indeed establish an antisense effect. Although PS-ONs were not degraded in the intracellular environment and are therefore not expected to spontaneously diffuse out of the cells, the fluorescence in the nuclei disappeared after more than 8 h. Interestingly, there seemed to be a fluorescence shift from the nucleus to the cytoplasm of the cells (Figure 3-12h): the nuclear fluorescence faded while fluorescent dots (as seen by confocal imaging) and simultaneous green and red fluorescence peaks (as seen by FCS) appeared in the cytoplasm of the cells. The identity of the cytoplasmic granules is currently unknown; however, their appearance directly correlates with the dissipation of the level of fluorescent ONs in the nucleus. This phenomenon has been observed previously by Fisher et al., who suggested that intracellular ONs could be exported from the cells by exocytosis (*16*). In agreement with Fisher et al., we believe that the formation of these cytoplasmic granules, which apparently contain the fluorescent ONs that were previously present in the nucleus, could indicate that the cells display an export pathway for removal of intact PS-ONs from the cells. It should be noted that nuclear bodies occurred in the nucleus before the apparent removal of the intact PS-ONs from the nuclei. Since the formation of nuclear bodies is reported to mainly occur at higher concentrations of PS-ONs (*14*−*16*), this could be the first step in exporting intact PS-ONs from the nuclei. Indeed, high PS-ON concentrations could trigger ordening of PS-ONs in nuclear bodies that are then exported via the cytoplasm to the cellular membrane. Whether the formation of nuclear bodies is correlated with the export of PS-ONs from the cells is an important question that remains to be elucidated.

As observed in this study, cellular entry and endosomal escape of ONs from the DOTAP/DOPE liposomes are not the major delivery bottlenecks as the transfected cells displayed fluorescent nuclei in the first hour following transfection. However, the efficient release of ONs at the time of endosomal escape does create a barrier for nuclease sensitive PO-ONs due to the rapid intracellular degradation of the naked PO-ONs. Therefore, carriers that could bring the PO-ONs as close as possible to the target mRNA or that allow the PO-ONs to establish an antisense effect while being encapsulated could be more suitable to delivery of unmodified PO-ONs. One such carrier that could do the trick is the cationic polymer polyethyleneimine (PEI). In general, it is believed that PEI escapes the endosomes via a proton sponge mechanism (*33*, *34*). The buffering capacity of PEI causes protons to be pumped in the endosomes, accompanied with an influx of Cl^- ions. This builds up the osmotic pressure which eventually causes the endosomes to rupture. The ON−PEI complexes are thus released in the cytosol of the cells as such, without release of the ONs at the step of endosomal escape. In contrast to liposome−DNA complexes, PEI−DNA complexes can enter the nucleus as an associated complex (*35*). Also, Pollard et al. (*36*) found that, in contrast to cationic lipids, the dissociation of plasmid DNA from PEI is not necessary for the establishment of a therapeutic effect, as was again observed recently by Honoré et al. (*37*). In a study employing oligonucleotides, Dheur et al. (*7*) observed that PEI was able to improve the antisense activity of nuclease sensitive PO-ONs while cationic lipids were not. We also observed that PO-ONs complexed with the cationic polymer *graft*-pDMAEMA [poly(2-dimethylamino)ethyl methacrylate-*co*-aminoethyl methacrylate-bearing polyethylene glycol chains] exhibited the same antisense effect as PS-ONs complexed with *graft*-pDMAEMA (*6*). These results support the idea that cationic polymers could exhibit more potential as nonviral gene delivery systems for unmodified ONs than cationic lipids.

As described in the introductory section, one approach to improving the antisense activity of nucleic acids is to synthesize ONs with increased nuclease stability so that intracellular degradation should not be an issue (*3*). However, modification of the ON backbone can introduce undesirable features such as solubility problems, delivery issues, a lack of RNase H activation, inactive isomers, or simply the cost of synthesis (*38*). Therefore, the development of cationic carriers that can efficiently deliver unmodified PO-ONs remains important and challenging. This study contributed to the understanding of the delivery problems of PO- and PS-ONs when complexed to DOTAP/DOPE liposomes, using FCS as a noninvasive tool to evaluate the distribution and stability of the ONs in the intracellular environment. We hope that the findings of this paper can strengthen the knowledge-based search for suitable delivery systems for realization of the therapeutic potential antisense therapy holds.

ACKNOWLEDGMENT

All experimental data were collected at the Advanced Light Microscopy Facility at the European Molecular Biology Laboratory (EMBL), Heidelberg, Germany. The lab of Rainer Pepperkok is gratefully acknowledged for the support during the visit of K.R. at the EMBL. We thank Leica Microsystems for continuous support of the Advanced Light Microscopy Facility.

REFERENCES

1. Sazani, P., and Kole, R. (2003) Therapeutic potential of antisense oligonucleotides as modulators of alternative splicing, *J. Clin. Invest. 112*, 481−486.
2. Holmlund, J. T. (2003) Applying antisense technology: Affinitak (TM) and other antisense oligonucleotides in clinical development, *Ther. Oligonucleotides 1002*, 244−251.

3. Agrawal, S. (1999) Importance of nucleotide sequence and chemical modifications of antisense oligonucleotides, *Biochim. Biophys. Acta 1489*, 53−68.
4. Brown, D. A., Kang, S. H., Gryaznov, S. M., Dedionisio, L., Heidenreich, O., Sullivan, S., Xu, X., and Nerenberg, M. I. (1994) Effect of Phosphorothioate Modification of Oligodeoxynucleotides on Specific Protein-Binding, *J. Biol. Chem. 269*, 26801−26805.
5. Pedroso de Lima, M. C., Simoes, S., Pires, P., Faneca, H., and Düzgünes, N. (2001) Cationic lipid-DNA complexes in gene delivery: From biophysics to biological applications, *Adv. Drug Delivery Rev. 47*, 277−294.
6. Lucas, B., Van Rompaey, E., Remaut, K., Sanders, N., De Smedt, S., and Demeester, J. (2004) On the biological activity of anti-ICAM-1 oligonucleotides complexed to non-viral carriers, *J. Controlled Release 96*, 207−219.
7. Dheur, S., Dias, N., van-Aerschot, A., Herdewijn, P., Bettinger, T., Remy, J. S., Helene, C., and Saison-Behmoaras, E. T. (1999) Polyethylenimine but not cationic lipid improves antisense activity of 3′-capped phosphodiester oligonucleotides, *Antisense Nucleic Acid Drug Dev. 9*, 515−525.
8. Shi, F., Nomden, A., Oberle, V., Engberts-Jan, B.-F. N., and Hoekstra, D. (2001) Efficient cationic lipid-mediated delivery of antisense oligonucleotides into eukaryotic cells: Down-regulation of the corticotropin-releasing factor receptor, *Nucleic Acids Res. 29*, 2079−2087.
9. Lucas, B., Remaut, K., Sanders, N. N., Braeckmans, K., De Smedt, S. C., and Demeester, J. (2005) Towards a better understanding of the dissociation behavior of liposome-oligonucleotide complexes in the cytosol of cells, *J. Controlled Release 103*, 435−450.
10. Lucas, B., Van-Rompaey, E., De-Smedt, S., Demeester, J., and Van-Oostveldt, P. (2002) Dual-color FFS to study the complexation between poly-L-lysine and oligonucleotides, *Macromolecules 35*, 8152−8160.
11. Remaut, K., Lucas, B., Braeckmans, K., Sanders, N. N., Demeester, J., and De Smedt, S. C. (2005) Protection of oligonucleotides against nucleases by pegylated and non-pegylated liposomes as studied by fluorescence correlation spectroscopy, *J. Controlled Release 110*, 209−223.
12. Remaut, K., Lucas, B., Braeckmans, K., Sanders, N. N., De Smedt, S. C., and Demeester, J. (2005) FRET-FCS as a tool to evaluate the stability of oligonucleotide drugs after intracellular delivery, *J. Controlled Release 103*, 259−271.
13. Jaaskelainen, I., Sternberg, B., Monkkonen, J., and Urtti, A. (1998) Physicochemical and morphological properties of complexes made of cationic liposomes and oligonucleotides, *Int. J. Pharm. 167*, 191−203.
14. Lorenz, P., Baker, B. F., Bennett, C. F., and Spector, D. L. (1998) Phosphorothioate antisense oligonucleotides induces the formation of nuclear bodies, *Mol. Biol. Cell 9*, 1007−1023.
15. Shoeman, R. L., Hartig, R., Huang, Y., Grueb, S., and Traub, P. (1997) Fluorescence microscopic comparison of the binding of phosphodiester and phosphorothioate (antisense) oligodeoxyribonucleotides to subcellular structures, including intermediate filaments, the endoplasmic reticulum, and the nuclear interior, *Antisense Nucleic Acid Drug Dev. 7*, 291−308.
16. Fisher, T. L., Terhorst, T., Cao, X. D., and Wagner, R. W. (1993) Intracellular Disposition and Metabolism of Fluorescently-Labeled Unmodified and Modified Oligonucleotides Microinjected Into Mammalian-Cells, *Nucleic Acids Res. 21*, 3857−3865.
17. Leonetti, J. P., Mechti, N., Degols, G., Gagnor, C., and Lebleu, B. (1991) Intracellular distribution of microinjected antisense oligonucleotides, *Proc. Natl. Acad. Sci. U.S.A. 88*, 2702−2706.
18. Chin, D. J., Green, G. A., Zon, G., Szoka, F. C., Jr., and Straubinger, R. M. (1990) Rapid nuclear accumulation of injected oligodeoxyribonucleotides, *New Biol. 2*, 1091−1100.
19. De Smedt, S. C., Remaut, K., Lucas, B., Braeckmans, K., Sanders, N. N., and Demeester, J. (2005) Studying biophysical barriers to DNA delivery by advanced light microscopy, *Adv. Drug Delivery Rev. 57*, 191−210.
20. Lucas, B., Remaut, K., Sanders, N. N., Braeckmans, K., De Smedt, S. C., and Demeester, J. (2005) Studying the intracellular dissociation of polymer-oligonucleotide complexes by dual color fluorescence fluctuation spectroscopy and confocal imaging, *Biochemistry 44*, 9905−9912.
21. Van Rompaey, E., Engelborghs, Y., Sanders, N., De Smedt, S. C., and Demeester, J. (2001) Interactions between oligonucleotides and cationic polymers investigated by fluorescence correlation spectroscopy, *Pharm. Res. 18*, 928−936.
22. Shi, F., and Hoekstra, D. (2004) Effective intracellular delivery of oligonucleotides in order to make sense of antisense, *J. Controlled Release 97*, 189−209.
23. Harashima, H., Shinohara, Y., and Kiwada, H. (2001) Intracellular control of gene trafficking using liposomes as drug carriers, *Eur. Pharm. Sci. 13*, 85−89.
24. Zelphati, O., and Szoka, F. C., Jr. (1996) Intracellular distribution and mechanism of delivery of oligonucleotides mediated by cationic lipids, *Pharm. Res. 13*, 1367−1372.
25. Zuhorn, I. S., Kalicharan, R., and Hoekstra, D. (2002) Lipoplex-mediated transfection of mammalian cells occurs through the cholesterol-dependent clathrin-mediated pathway of endocytosis, *J. Biol. Chem. 277*, 18021−18028.
26. Zelphati, O., and Szoka, F. C., Jr. (1996) Mechanism of oligonucleotide release from cationic liposomes, *Proc. Natl. Acad. Sci. U.S.A. 93*, 11493−11498.
27. Gordon, S. P., Berezhna, S., Scherfeld, D., Kahya, N., and Schwille, P. (2005) Characterization of interaction between cationic lipid-oligonucleotide complexes and cellular membrane lipids using confocal imaging and fluorescence correlation spectroscopy, *Biophys. J. 88*, 305−316.
28. Fattal, E., Couvreur, P., and Dubernet, C. (2004) "Smart" delivery of antisense oligonucleotides by anionic pH-sensitive liposomes, *Adv. Drug Delivery Rev. 56*, 931−946.
29. Zuhorn, I. S., Bakowsky, U., Polushkin, E., Visser, W. H., Stuart, M. C. A., Engberts, J. B. F. N., and Hoekstra, D. (2005) Nonbilayer phase of lipoplex-membrane mixture determines endosomal escape of genetic cargo and transfection efficiency, *Mol. Ther. 11*, 801−810.
30. Marcusson, E. G., Bhat, B., Manoharan, M., Bennett, C. F., and Dean, N. M. (1998) Phosphorothioate oligodeoxyribonucleotides dissociated from cationic lipids before and entering the nucleus, *Nucleic Acids Res. 26*, 2016−2023.
31. Uchiyama, H., Hirano, K., Kashiwasake-Jibu, M., and Taira, K. (1996) Detection of Undegraded Oligonucleotides *in Vivo* by Fluorescence Resonance Energy Transfer, *J. Biol. Chem. 271*, 380−384.
32. Woolf, T. M., Jennings, C. G. B., Rebagliati, M., and Melton, D. A. (1990) The Stability, Toxicity and Effectiveness of Unmodified and Phosphorothioate Antisense Oligodeoxynucleotides in *Xenopus* Oocytes and Embryos, *Nucleic Acids Res. 18*, 1763−1769.
33. Godbey, W. T., Wu, K. K., and Mikos, A. G. (1999) Poly(ethylenimine) and its role in gene delivery, *J. Controlled Release 60*, 149−160.
34. Bieber, T., Meissner, W., Kostin, S., Niemann, A., and Elsasser, H. (2002) Intracelullar route and transcriptional competence of polyethylenimine-DNA complexes, *J. Controlled Release 82*, 441−454.
35. Godbey, W. T., Wu, K. K., and Mikos, A. G. (1999) Tracking the intracellular path of poly(ethylenimine)/DNA complexes for gene delivery, *Proc. Natl. Acad. Sci. U.S.A. 96*, 5177−5181.
36. Pollard, H., Remy, J. S., Loussouarn, G., Demolombe, S., Behr, J. P., and Escande, D. (1998) Polyethylenimine but not cationic lipids promotes transgene delivery to the nucleus in mammalian cells, *J. Biol. Chem. 273*, 7507−7511.
37. Honoré, I., Grosse, S., Frison, N., Favatier, F., Monsigny, M., and Fajac, I. (2005) Transcription of plasmid DNA: Influence of plasmid DNA/polyethyleneimine complex formation, *J. Controlled Release* (in press).
38. Hogrefe, R. I. (1999) An antisense oligonucleotide primer, *Antisense Nucleic Acid Drug Dev. 9*, 351−357.

BI0519755